Asymmetric Self-Phase Modulation and Compression of Short Laser Pulses in Plasma Channels

D. F. Gordon and B. Hafizi
Icarus Research, Inc., P.O. Box 30780, Bethesda, Maryland 20824-0780, USA

R. F. Hubbard, J. R. Peñano, P. Sprangle, and A. Ting
Plasma Physics Division, Naval Research Laboratory, Washington, D.C. 20375, USA
(Received 13 November 2002; published 30 May 2003)

A relativistically intense femtosecond laser pulse propagating in a plasma channel undergoes dramatic photon deceleration while propagating a distance on the order of a dephasing length. The deceleration of photons is localized to the back of the pulse and is accompanied by compression and explosive growth of the ponderomotive potential. Fully explicit particle-in-cell simulations are applied to the problem and are compared with ponderomotive guiding center simulations. A numerical Wigner transform is used to examine local frequency shifts within the pulse and to suggest an experimental diagnostic of plasma waves inside a capillary.

DOI: 10.1103/PhysRevLett.90.215001 PACS numbers: 52.35.Mw, 42.65.Jx, 52.38.Dx, 52.38.Kd

Guiding of intense short laser pulses in preformed plasma channels [1–4] has potential applications in the areas of plasma-based accelerators [5–7], x-ray lasers [8–10], and harmonic generation [11,12]. For example, in the laser wakefield accelerator (LWFA) a relativistically intense laser pulse is used to drive large amplitude plasma waves which can be used to rapidly accelerate electrons. Without guiding, the acceleration distance would be limited by the Rayleigh length of the driving laser pulse. With guiding, the acceleration distance can be extended to the classical dephasing length [7,13]

$$L_d = 2\pi c/[4\omega_p(1-\beta_g)],$$

where ω_p is the plasma frequency and $\beta_g c$ is the group velocity of the laser pulse. The dephasing length turns out to be a useful length scale over which to consider the nonlinear evolution of the laser pulse.

In the case where the pulse is longer than a plasma period, Raman and modulational instabilities can lead to disruption of the pulse [14,15]. In the case where the pulse is shorter than a plasma period, it is not yet clear what mode of pulse distortion might develop. Esarey *et al.* [16] predicted steepening at the front of the laser pulse but dropped an important term from the wave equation. Sprangle *et al.* [17] included the missing term in a weakly relativistic theory and predicted steepening at the back of the pulse. A more dramatic compression effect was noted in [13]. Pulse compression in a uniform plasma was discussed in [18,19]. In this Letter, we describe fully relativistic simulations and an accompanying analysis which identify the key nonlinear behavior of a short pulse propagating in a plasma channel. We find that the pulse stretches in the front and compresses in the back. The distortions grow explosively rather than exponentially and are accompanied by large localized frequency downshifts.

Photon kinetic theory [20,21] offers a heuristic picture of pulse propagation in a plasma. The theory begins with a Wigner transform of the laser field which gives the photon number density in classical phase space. Using SI units, this becomes in one dimension [21]

$$N(x,k) = \frac{\epsilon_0}{8\hbar}\left(\frac{\partial D}{\partial\omega}\right)_{\omega_0} F(x,k),$$

where $D = 1 - \omega_p^2/\omega^2 - c^2k^2/\omega^2$ is the plasma dispersion function, ϵ_0 is the permittivity of free space, and

$$F(x,k) = \int E(x - s/2)E^*(x + s/2)e^{iks}ds.$$

Here E is the complex laser electric field and k is the wave number. In the limit of short wavelength, it can be shown that N satisfies a Vlasov equation and, therefore, represents a collection of photons with definite positions, frequencies, and wave numbers. The velocity of a photon is the group velocity evaluated at the frequency of the photon. Thus, frequency shifts in the laser pulse can be formally identified with the acceleration of a particular element of the photon phase space. This leads naturally to the term "photon acceleration" [22], which is the photon kinetic analog of self-phase modulation.

Using the photon kinetic picture, it can be easily shown that a laser pulse propagating in an underdense plasma must decelerate. Let the normalized vector potential of the laser $\tilde{a} = |e|A/mc^2$ be expressed in the form $\tilde{a} = \frac{1}{2}a\exp(-i\omega_0\xi) + \text{c.c.}$, where ω_0 is the center frequency of the laser normalized to ω_p and $\xi = \omega_p(x/c - t)$ measures axial position in the speed of light frame. In the underdense limit, a then satisfies [23,24]

$$(\nabla_\perp^2 - 2i\omega_0\partial_t + 2\partial_{t\xi})a = -j, \qquad (1)$$

where j is the envelope of the rapidly varying current density. Under the approximation of Eq. (1) photon number is conserved [25]. Combining this with the fact that the laser pulse must lose energy shows that more photons lose energy than gain it. Thus, for most photons the group velocity is reduced and the laser pulse decelerates. The validity of Eq. (1) will be demonstrated below.

Photon deceleration occurs when the refractive index increases with time at a fixed point in space. In the limit of $a \ll 1$, the nonlinear contribution to the refractive index of a tenuous plasma is [22,26]

$$\delta\eta \approx \frac{|a|^2/4 - \delta n}{2\omega_l^2},$$

where δn is the density perturbation normalized to the ambient density and ω_l is the local frequency normalized to ω_p. The $|a|^2/4$ term results from the change in the mass of the electrons as they quiver in the laser field. Sprangle *et al.* [17] pointed out that for a broad beam, δn tends to cancel $|a|^2/4$ in the limit of a short pulse with $a \ll 1$. The simulations presented here indicate that this cancellation becomes progressively less effective toward the back of a pulse. For a resonant wakefield driver with a pulse length of π/ω_p, the slope of $\delta\eta(\xi)$ is negative throughout most of the pulse. As illustrated below, this causes almost all photons to decelerate, with the largest shifts occurring in the tail of the pulse. This contrasts with ordinary nonlinear optics where the frequency shift is antisymmetric about the pulse center. Here, the symmetry is broken because of the fact that the pulse constantly loses energy to plasma waves.

An estimate of how far a short pulse can propagate before nonlinear effects become important has been derived by Bulanov *et al.* [25]. Defining $Q \equiv \int |a|^2 d\xi$, and assuming $|a| \gg 1$, it was found that

$$Q(t) = Q(0)(1 - t/t_{nl})^{-1/3}, \tag{2}$$

where $t_{nl} = (16/3)[c/Q(0)](\omega_0^2/\omega_p^4)$ and $t < t_{nl}$. When the pulse length is π/ω_p, the nonlinear evolution time can be expressed very simply in terms of the dephasing length:

$$ct_{nl} \approx \frac{L_d}{2|a|^2}. \tag{3}$$

Although these relations assume $|a| \gg 1$, we have recovered the functional form of Eq. (2) very accurately in several 1D simulations with $|a| \lesssim 1$. The same simulations showed that t_{nl} can be estimated to well within an order of magnitude by Eq. (3). The simulations discussed below show that the same results hold for propagation in a plasma channel and that the *peak* value of $|a|^2$ follows a $(1 - t/t_{nl})^{-1/2}$ dependence. For $|a| \lesssim 1$, this corresponds to explosive growth of the ponderomotive potential.

Two simulation models will be utilized in this Letter, both of which are contained within the massively parallel framework of turboWAVE [24]. The first is a standard fully explicit particle-in-cell model which is electrodynamically exact in the limit of infinitesimal grid spacing. The second is a recently developed "ponderomotive guiding center fluid model" (PGC-F) which is valid in the limit $\omega_0 \gg \omega_p$. In this model, the laser radiation is described by the envelope Eq. (1). The wakefields are updated using the exact Maxwell equations. The sources are computed by solving for the cycle averaged motions of a cold electron fluid using $\partial_t \mathbf{p} = -\mathbf{E} - \nabla\bar{\gamma}$, where $\mathbf{p}$ is the momentum of a fluid element, $\mathbf{E}$ is the wake electric field, and $\bar{\gamma} = \sqrt{1 + |\mathbf{p}|^2 + |a|^2/2}$. This equation can be derived from the time averaged kinetic equation of motion discussed in Ref. [23]. Finally, the electron density n is computed by integrating the continuity equation using a flux conserving algorithm, and the laser induced current density is computed from $j = -na/\bar{\gamma}$.

We first establish using 1D simulations that the PGC-F model agrees with the fully explicit model. We then consider 2D simulations using only the computationally inexpensive PGC-F model. This procedure is justified because the assumptions of the PGC-F model are strained primarily by frequency shifts which do not result from transverse derivatives.

The physical parameters to be considered for all the simulations in this Letter correspond to a LWFA utilizing a capillary discharge [2] to create the plasma channel. The on-axis electron density is $n_0 = 8 \times 10^{17}$ cm^{-3}. This gives the resonant laser pulse length as $\tau_L = 60$ fs, where τ_L is the full width at half maximum and the pulse shape is the one described in Ref. [24]. Transversely, the laser is described by $a(r) = a_0 \exp(-r^2/r_0^2)$, where $a_0 = 0.7$ and $r_0 = 30$ μm. This requires 15 TW of laser power given a wavelength of 0.8 μm. These parameters are well within the reach of modern laser technology. Finally, the transverse density variation is given by $n(r) = n_0(1 + r^2/r_{ch}^2)$, where $r_{ch} = 76$ μm. This profile corresponds to the matched beam condition [13] and keeps the spot size constant as the pulse propagates.

For the 1D fully explicit simulation, there were 8192 cells and 9×10^6 time steps. For the 1D PGC-F simulation, there were 1024 cells and 1.4×10^6 time steps. In both cases, the computational region was set in motion at the speed of light. The results are illustrated in Fig. 1. Figure 1(a) shows $|a(\xi)|^2$ before the interaction. Figures 1(b) and 1(c) show $|a(\xi)|^2$ at the point of maximum compression as computed by the fully explicit and PGC-F models, respectively. In both cases, maximum compression occurred after a propagation distance of $2.6L_d$ (9 cm). Compression occurred in the tail, with $|a|^2$ amplifying by a factor of 4. The intensity amplification was only twofold, suggesting that frequency shifts contributed to the increase in $|a|^2$. The intensity is of less interest than $|a|^2$ in cases where the ponderomotive force is important. Figure 1(d) shows the growth of the peak $|a|^2$ as a function of the propagation distance ct. The solid line is data from the fully explicit simulation, and the dashed line is a least squares fit to a function of the

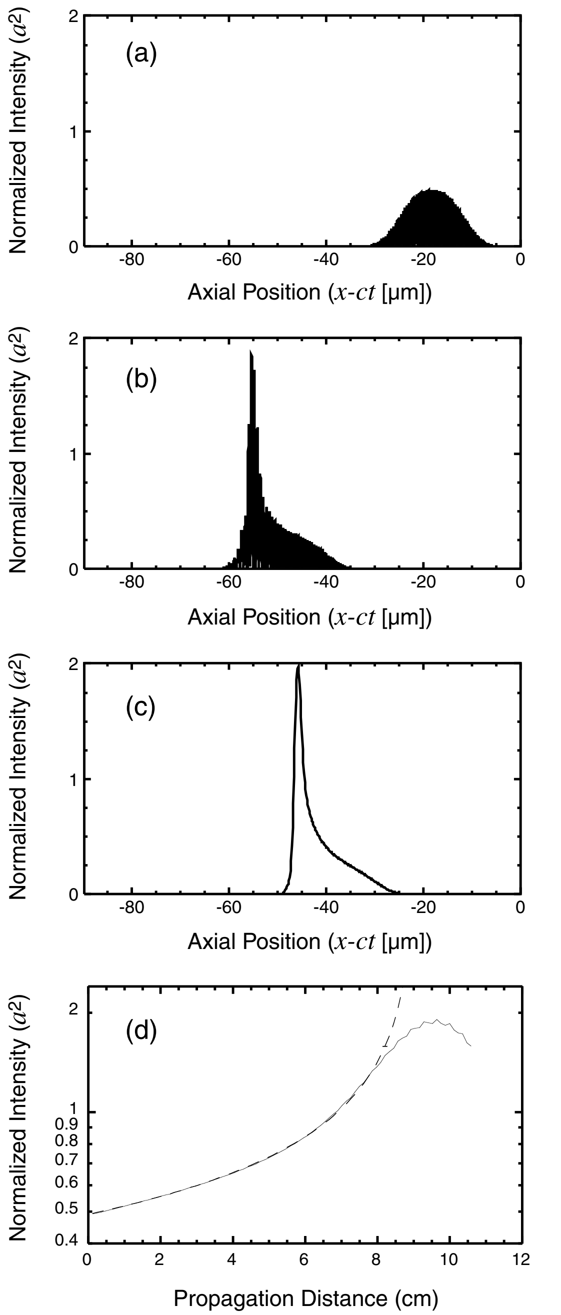

FIG. 1. 1D simulations of propagation of a laser pulse with $a = 0.7$ and $\tau_L = 60$ fs. The front of the pulse is on the right. (a) $|a|^2$ vs $x - ct$ before the interaction, (b) $|a|^2$ vs $x - ct$ after 9 cm propagation using the fully explicit model, and (c) $|a|^2$ vs $x - ct$ after 9 cm propagation using the PGC-F model. (d) The solid line shows explosive growth of the peak $|a|^2$ with ct as computed by the fully explicit model, and the dashed line is the function $0.489(1 - ct/9.05)^{-1/2}$.

form $a_0^2(1 - t/t_{nl})^{-1/2}$. The best fit occurs for $a_0^2 = 0.489$ and $ct_{nl} = 9.05$ cm. It was verified empirically that an exponent of $-1/2$ minimizes the error.

One noticeable discrepancy between the fully explicit simulation and the PGC-F simulation is that the fully explicit simulation predicted a larger group delay. This is because in the fully explicit model numerical dispersion increases with frequency, while in the PGC-F model it increases with the shift from the center frequency. It is also worth noting that approximately five grid cells per optical cycle were required to obtain convergence in the PGC-F simulation.

For the 2D simulation, there were 1024×128 cells and 1.2×10^6 time steps. The results are shown in Fig. 2. Figure 2(a) shows on-axis lineouts of $|a|^2/8\omega_0^2$ and $\delta\eta$ early in the interaction. The lineout of $|a|^2/8\omega_0^2$ measures the relativistic contribution to $\delta\eta$ and also indicates the location of the pulse. As predicted in Ref. [17], the total nonlinearity is much smaller than the relativistic contribution alone near the head of the pulse. However, throughout most of the pulse, $\delta\eta$ increases monotonically from head to tail. This causes phase fronts to separate leading to photon deceleration. Group velocity dispersion then causes photons to bunch near the tail of the pulse. This is illustrated in Fig. 2(b), which shows an intensity plot of $|a(\xi, y)|^2$ after 9 cm of propagation. As in the 1D case, compression and amplification occur in the tail of the pulse. However, the degree of compression is slightly less, with the peak $|a|^2$ reaching about 90% of the value it reached in the 1D PGC-F simulation.

The Wigner transform of the on-axis electric field of the laser after 9 cm of propagation is shown in Fig. 2(c). The conventional spectrum can be recovered by integrating over the spatial coordinate. The red area reminiscent of a check mark indicates the highest concentration of photons. As foretold, most of the photons are downshifted and, hence, decelerated. Furthermore, the downshift increases with distance from the head of the pulse, and at its maximum is on the order of the carrier frequency itself. The correlation between speed and position suggests that the pulse will stretch with further propagation. This is consistent with the fact that the data are evaluated at the point of maximum compression. The blue areas are regions where the photon number density is negative. The appearance of negative numbers is a reflection of the fact that the wave aspect of the light cannot be entirely neglected.

The distinctive appearance of Fig. 2(c) suggests that frequency resolved optical gating (FROG) [27] could be used as an experimental indicator of plasma wave excitation inside a capillary. To check this, we have generated a numerical FROG trace based on simulation data and recovered an image very similar to Fig. 2(c). The inference that plasma waves were excited would be particularly strong since the asymmetry in the frequency shifts is fundamentally related to the deposition of laser energy into collective modes of the plasma.

Finally, Fig. 2(d) shows the growth of the peak $|a|^2$ as a function of propagation distance. The curve is once again approximated very well by a function of the form $a_0^2(1 - t/t_{nl})^{-1/2}$. For this case, $a_0^2 = 0.552$ and

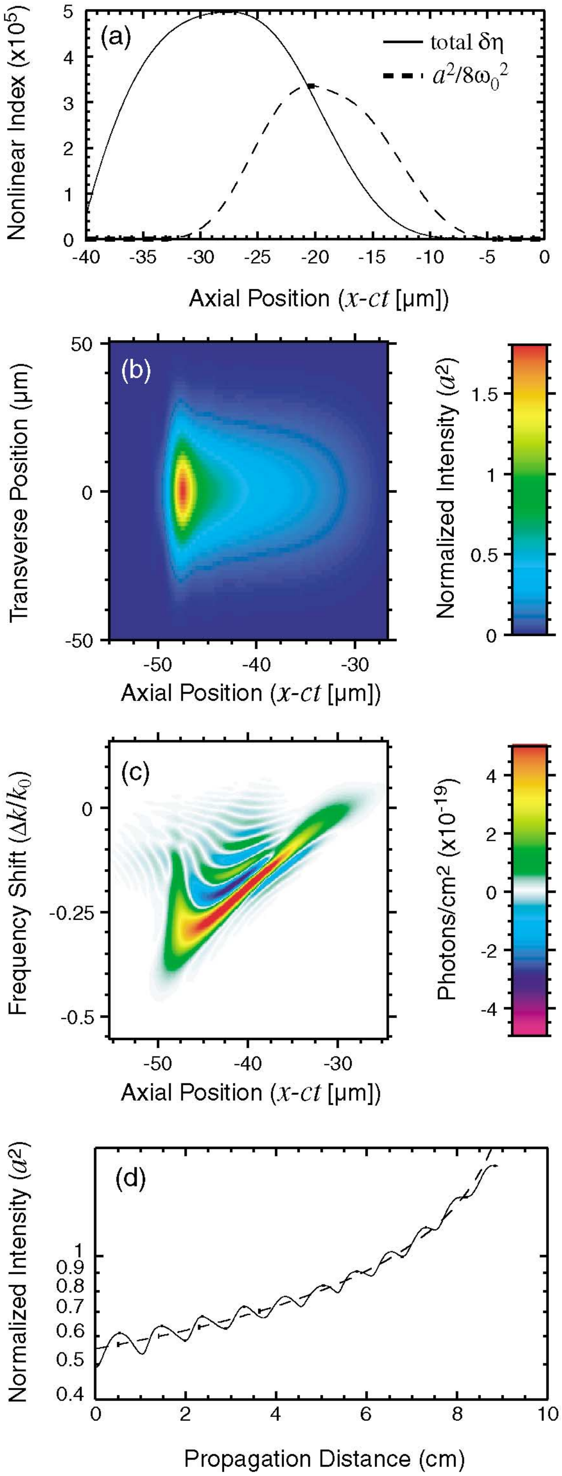

FIG. 2 (color). 2D simulation of a channel guided laser pulse with $a = 0.7$ and $\tau_L = 60$ fs. (a) On-axis contributions to the nonlinear refractive index early in the interaction. The dashed line is $|a|^2/8\omega_0^2$ and the solid line is $\delta\eta$. (b) Intensity plot of $|a(x, y)|^2$ after 9 cm. (c) Wigner transform of the on-axis electric field of the laser showing local frequency content. Here $\Delta k = k - k_0$, where $k_0 = \omega_0\omega_p/c$ (ω_0 is dimensionless). (d) The solid line is $|a|^2$ vs ct as computed by simulation and the dashed line is the function $0.552(1 - ct/9.49)^{-1/2}$.

$ct_{nl} = 9.49$ cm. The oscillations in the simulated $|a|^2$ are due to a small mismatch between the laser spot size and the channel radius.

In conclusion, short laser pulses such as those used in a resonantly driven LWFA are subject to dramatic compression and deceleration after propagating a distance of two or three classical dephasing lengths. The associated distortions grow explosively rather than exponentially. For LWFA applications, pulse compression could be beneficial because of the associated intensity enhancement, but photon deceleration will shorten the dephasing length. Furthermore, by comparing experimentally and numerically obtained FROG traces it may be possible to infer the excitation of plasma waves inside a channel.

We acknowledge useful discussions with A. Zigler and P. Schuck. This work was supported by a DOE Small Business Innovation Research (SBIR) Grant to Icarus Research, Inc. A portion of this work was also supported by the Division of High Energy Physics, Office of Energy Research, U.S. Department of Energy and by the Office of Naval Research.

[1] H. Milchberg *et al.*, Phys. Plasmas **3**, 2149 (1996).
[2] D. Kaganovich *et al.*, Phys. Rev. E **59**, R4769 (1999).
[3] P. Volfbeyn *et al.*, Phys. Plasmas **6**, 2269 (1999).
[4] E. Gaul *et al.*, Appl. Phys. Lett. **77**, 4112 (2000).
[5] T. Tajima and J. M. Dawson, Phys. Rev. Lett. **43**, 701 (1979).
[6] D. Umstadter, Phys. Plasmas **8**, 1774 (2001).
[7] E. Esarey *et al.*, IEEE Trans. Plasma Sci. **24**, 252 (1996).
[8] D. Eder *et al.*, Phys. Plasmas **1**, 1774 (1994).
[9] J. Rocca *et al.*, Phys. Rev. Lett. **73**, 2192 (1994).
[10] D. Korobkin *et al.*, Phys. Rev. Lett. **77**, 5206 (1996).
[11] H. Milchberg *et al.*, Phys. Rev. Lett. **75**, 2494 (1995).
[12] A. Rundquist *et al.*, Science **280**, 1412 (1998).
[13] R. Hubbard *et al.*, IEEE Trans. Plasma Sci. **28**, 1122 (2000).
[14] G. Shvets and X. Li, Phys. Plasmas **8**, 8 (2001).
[15] J. Peñano *et al.*, Phys. Rev. E **66**, 036402 (2002).
[16] E. Esarey *et al.*, Phys. Rev. Lett. **84**, 3081 (2000).
[17] P. Sprangle *et al.*, Phys. Rev. E **63**, 056405 (2001).
[18] C. Ren *et al.*, Phys. Rev. E **63**, 026411 (2001).
[19] M. Lontano and I. G. Murusidze, Opt. Express **11**, 248 (2003).
[20] I. Besieris and F. Tappert, J. Math. Phys. (N.Y.) **17**, 734 (1976).
[21] L. Silva and J. Mendonca, Phys. Rev. E **57**, 3423 (1998).
[22] W. B. Mori, IEEE J. Quantum Electron. **33**, 1942 (1997).
[23] P. Mora and T. Antonsen, Phys. Plasmas **4**, 217 (1997).
[24] D. F. Gordon *et al.*, IEEE Trans. Plasma Sci. **28**, 1224 (2000).
[25] S. Bulanov *et al.*, Phys. Fluids B **4**, 1935 (1992).
[26] A. Ting *et al.*, in *Advanced Accelerator Concepts*, edited by Chan Joshi, AIP Conf. Proc. No. 193 (AIP, New York, 1989), pp. 398–407.
[27] D. J. Kane and R. Trebino, Opt. Lett. **18**, 823 (1993).